Effect of Aerosols on the Transfer of Solar Energy Through Realistic Model Atmospheres. Part II: Partly-Absorbing Aerosols

NORMAN BRASLAU

IBM T. J. Watson Research Center, Yorktown Heights, N. Y. 10598

AND J. V. DAVE

IBM Scientific Center, Palo Alto, Calif. 94304

(Manuscript received 16 January 1973, in revised form 9 March 1973)

ABSTRACT

Results are presented of an extensive theoretical investigation aimed at evaluating the effect of changing the refractive index of the aerosol substance from 1.5–0*i* to 1.5–0.01*i* on the solar energy absorbed, reflected and transmitted by cloudless, plane-parallel, nonhomogeneous atmospheric models.

1. Introduction

In Part I (Braslau and Dave, 1973a) we presented results of calculations aimed at determining the effect of non-absorbing (refractive index $m=1.5\text{–}0i$) aerosols on the solar radiation transfer by cloudless, nonhomogeneous, plane-parallel atmospheric models. The concentration of aerosols (spherical particles with size distribution and refractive index independent of height), ozone and water vapor were specified for 160 layers of varying thickness from the surface to 45 km. The solar spectrum (0.285–2.5 μm) containing 96.1% of the total solar energy incident on the top of the atmosphere, was divided into 83 intervals with appropriate functions representing the scattering and absorption of gases and aerosol assigned to each, the index of refraction of the aerosol taken to be wavelength-independent. Upward and downward fluxes for each spectral interval at each level were computed taking into account all orders of scattering. Results were presented for four model atmospheres to show variations of the absorbed, diffusely reflected, and diffusely as well as directly transmitted spectrally integrated solar flux as a function of Lambert ground reflectivity (R), and solar zenith angle (θ_0).

TABLE 1. Percent of the incident solar energy directly transmitted by the various atmospheric models.

Model	Solar zenith angle 0°	30°	60°	80°
C	72.25	69.82	58.72	31.32
C1	72.32	69.89	58.81	31.42
D	54.57	50.52	33.76	7.09
D1	54.71	50.66	33.91	7.15

In this second part, we report the extension of this work to the effect of partly-absorbing ($m=1.5\text{–}0.01i$) aerosols on the solar energy transfer. In particular, we shall compare variations of the fore-mentioned quantities as a function of R and θ_0 when the atmospheric dust in Models C and D (Braslau and Dave, 1973a) is changed from non-absorbing to partly-absorbing. It may be noted that Models C and D, both with atmospheric gases distributed according to average mid-latitude summer conditions (McClatchey *et al.*, 1970), respectively, contain "Average" and "Heavy" dust distribution displayed in Fig. 2 of Part I. The assumed size distribution for the aerosols is the one referred to as haze L by Deirmendjian (1969). The new models C and D with partly-absorbing aerosols will be referred to as C1 and D1, respectively.

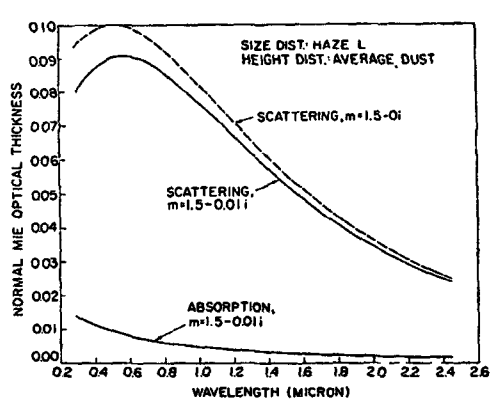

FIG. 1. Normal Mie optical thickness due to scattering and absorption by spherical aerosols of two different refractive indices: size distribution, haze L (Deirmendjian, 1969); height distribution, "Average" dust (Fig. 2, Part I, Braslau and Dave, 1973).

The theory developed in Part I is valid for aerosol with a complex index of refraction. A new magnetic tape containing Legendre coefficients used for computing the Mie scattering functions is required for the complex index of refraction used in this work. The calculation then proceeds as described in Part I, with no other alterations in the programs.

2. Discussion of results

a. Directly transmitted solar flux

From values of the solar energy directly transmitted by Models C, C1, D and D1 given in Table 1, it can be seen that an increase in the imaginary part (n_2) of the refractive index from 0.0 to 0.01 results in a small but significant increase of the direct solar radiation received by the surface. The reasons for this can be found in Fig. 1 where variations of the normal Mie-scattering and Mie-absorption optical thicknesses are depicted as a function of wavelength (λ) for Models C (broken curve) and C1 (solid curve). The Mie-absorption optical thickness for Model C is zero. An increase in n_2 results in a moderate decrease in the scattering optical thickness of the aerosols at shorter wavelengths. In fact, the total (scattering and absorption) aerosol optical thickness for Model C1 is smaller than that for Model C by a small but significant amount ($\sim$0.5%) in the spectral region 0.285–1.395 μm. Since this is the region containing most energy, we have an overall increase in transparency of the atmosphere for direct radiation when aerosols are changed from non-absorbing to partly-absorbing.

b. Net flux

Variations of the spectrally integrated net (downward−upward) solar flux for $\theta_0=80°$ and for all four models are displayed as a function of height in Figs. 2 and 3 for $R=0$ and 0.8, respectively. An increase in the imaginary part of the refractive index from 0.0 to 0.01 results in an increase in net flux at the top of the atmosphere, but in a decrease at the surface. This is due to a decrease in planetary albedo and skylight flux (Section 2c) from additional absorption of solar energy by the aerosols. For $R=0$, the amount of energy absorbed by the whole atmosphere increases by about 11% and 36% as we change from Models C and D to Models C1 and D1, respectively. For $R=0.8$, the corresponding figures are 12% and 41%. However, this increase is not distributed uniformly over all levels. This is because the prime absorbers for Models C and D are ozone and water vapor, while the other two models

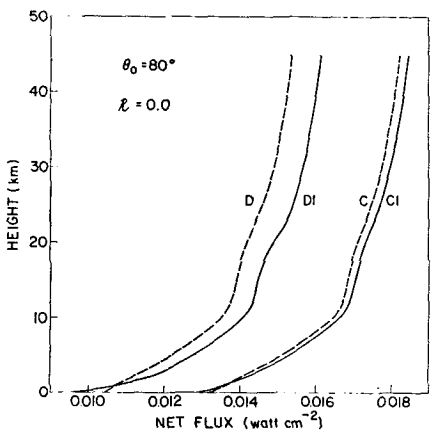

FIG. 2. Spectrally integrated net flux as a function of height for the four models described in Section 1: $\theta_0=80°$, $R=0$.

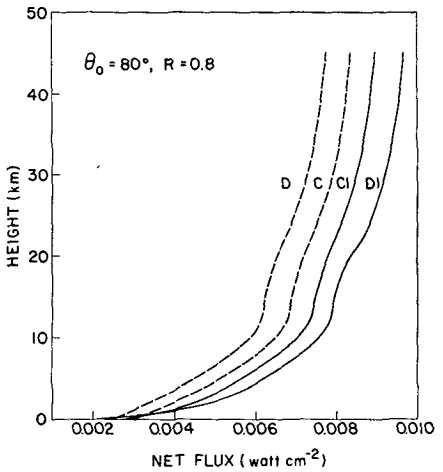

FIG. 3. Same as Fig. 2 but for $R=0.8$.

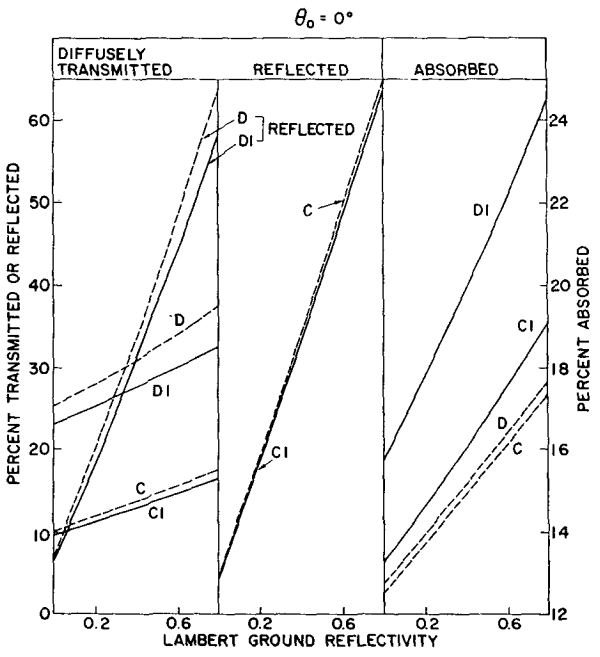

FIG. 4. Percent of the incident solar energy (0.285–2.5 μm) diffusely transmitted and reflected, as well as absorbed by the model atmospheres, as a function of Lambert ground reflectivity of the underlying ground: $\theta_0=0°$.

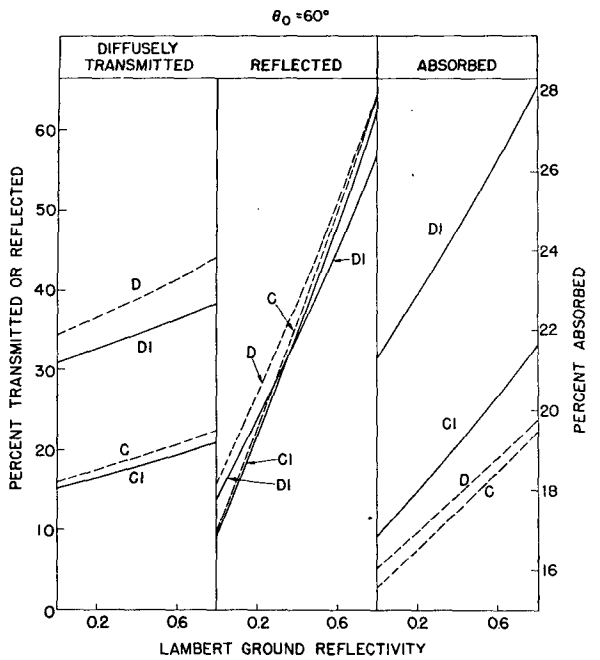

FIG. 5. Same as Fig. 4 but for $\theta_0=60°$.

contain additional absorption due to aerosols. Furthermore, concentration of each of these varies in a different manner with height.

The net flux vs height curves for Models C and D run parallel to those for C1 and D1, respectively, in the region 45–25 km, as the aerosol content of this region is less than 0.2% of the total. Consequently, absorption in this part of the atmosphere is due to ozone only.

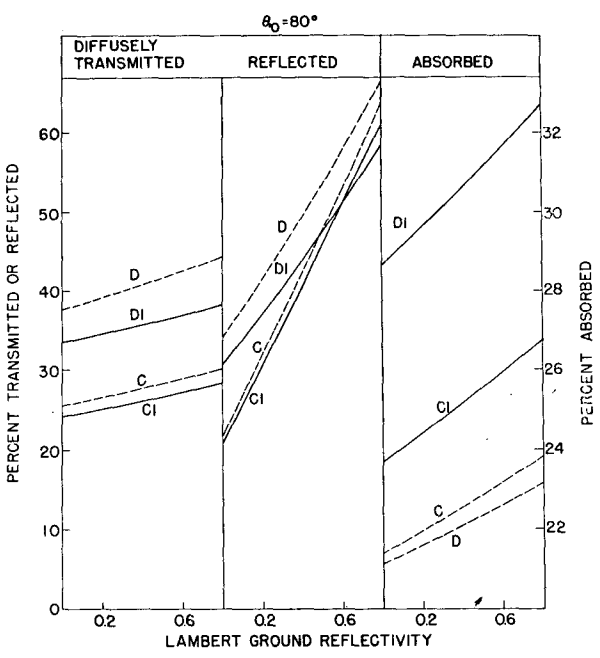

FIG. 6. Same as Fig. 4 but for $\theta_0=80°$.

TABLE 2. Percent of the incident solar energy diffusely transmitted by the various atmospheric models.

Solar zenith angle	Model	Lambert ground reflectivity 0.0	0.05	0.1	0.2	0.3	0.4	0.6	0.8
0°	C1	9.63	10.00	10.38	11.15	11.95	12.78	14.53	16.44
	D1	23.11	23.62	24.13	25.18	26.27	27.40	29.77	32.35
30°	C1	10.67	11.03	11.39	12.15	12.92	13.73	15.44	17.31
	D1	24.87	25.36	25.85	26.87	27.92	29.01	31.31	33.79
60°	C1	15.16	15.48	15.81	16.48	17.17	17.89	19.41	21.05
	D1	30.78	31.19	31.61	32.47	33.36	34.28	36.22	38.31
80°	C1	24.17	24.40	24.64	25.12	25.61	26.12	27.19	28.35
	D1	33.58	33.84	34.10	34.64	35.20	35.78	37.00	38.31

Another region which is least affected by increase in the value of n_2 is the one bounded by the 5- and 12-km levels, and containing about 1.6% (for the Model C) of the total aerosol content of the entire vertical column. On the other hand, increased aerosol absorption results in a 5–27% increase in the amount of energy absorbed by the lower stratosphere (12–25 km region), and in a 25–92% increase for the lower tropospheric region (0–5 km) depending upon the model and reflectivity of the underlying surface. Detailed tables of flux components at kilometer intervals for these models are available elsewhere (Braslau and Dave, 1972).

c. *Variations with ground reflectivity*

The quantities which are of primary importance in investigations of the climatological effect of atmospheric dust loadings are the percent of the total incident flux transmitted to the ground, reflected back to space (planetary albedo), and absorbed in the atmosphere, together with the cooling rate which is proportional to the derivative of net flux with respect to height. Variations of the directly transmitted flux with θ_0 were discussed in Section 2a. Variations of the remaining three fluxes (*viz.* diffusely transmitted, absorbed and reflected) as a function of the Lambert ground reflectivity (R) of the surface underlying the model are displayed in Figs. 4–6 for $\theta_0=0°$, 60° and 80°, respectively. Numerical values of all three quantities for $\theta_0=0°$, 30°, 60° and 80°, and for $R=0$, 0.05, 0.1, 0.2, 0.3, 0.4, 0.6

TABLE 3. Percent of the incident solar energy diffusely reflected by the various atmospheric models.

Solar zenith angle	Model	Lambert ground reflectivity 0.0	0.05	0.1	0.2	0.3	0.4	0.6	0.8
0°	C1	4.84	8.24	11.67	18.62	25.69	32.90	47.74	63.20
	D1	6.48	9.38	12.33	18.33	24.49	30.82	44.02	58.01
30°	C1	5.54	8.89	12.27	19.12	26.09	33.19	47.81	63.04
	D1	7.65	10.48	13.34	19.18	25.18	31.34	44.18	57.79
60°	C1	9.22	12.33	15.47	21.82	28.28	34.86	48.40	62.48
	D1	14.02	16.47	18.95	24.01	29.20	34.52	45.63	57.38
80°	C1	20.73	23.11	25.51	30.37	35.30	40.32	50.63	61.33
	D1	30.63	32.19	33.78	37.00	40.31	43.71	50.79	58.27

TABLE 4. Percent of the incident solar energy absorbed by the various atmospheric models.

Solar zenith angle	Model	Lambert ground reflectivity 0.0	0.05	0.1	0.2	0.3	0.4	0.6	0.8
0°	C1	13.21	13.55	13.90	14.61	15.32	16.05	17.52	19.05
	D1	15.70	16.21	16.72	17.76	18.83	19.92	22.19	24.58
30°	C1	13.90	14.24	14.57	15.25	15.94	16.64	18.06	19.52
	D1	16.82	17.31	17.80	18.79	19.81	20.86	23.03	25.32
60°	C1	16.81	17.10	17.38	17.95	18.53	19.12	20.32	21.55
	D1	21.29	21.68	22.08	22.89	23.71	24.56	26.32	28.18
80°	C1	23.68	23.86	24.04	24.41	24.78	25.16	25.93	26.72
	D1	28.64	28.87	29.10	29.56	30.04	30.53	31.55	32.63

and 0.8 are given in Tables 2–4 for Models C1 and D1. Similar tables for the Models C and D can be found in Part I of this paper.

For $\theta_0=0°$, increase in the value of n_2 from 0 to 0.01 results in a decrease in diffusely transmitted component by about 0.6 and 2.3% for Models C and D, respectively, when $R=0$, and by about 1.2 and 5.0% when respective models rest on a Lambert ground with $R=0.8$. Increased aerosol absorption leads to a significant decrease in planetary albedo only when the ground reflectivity is high, and/or the dust content is high. The amount of energy absorbed by the atmosphere increases by 0.7 and 3.0%, respectively, as the aerosols in Models C and D resting on a non-reflecting surface are converted from non-absorbing to partly-absorbing. The corresponding increases for the case where models rest on a ground with Lambert reflectivity of 0.8 are 1.7 and 6.9%.

As the solar zenith angle of the sun is increased from 0° to 80° (Figs. 4–6), the percentage of the incident flux transmitted to the ground, absorbed in the atmosphere, and reflected to space all show an increasingly stronger dependence on the imaginary part of the refractive index of the aerosol substance.

As in Part I, these spectrally integrated fluxes were obtained by summing the contributions from 83 unequal spectral intervals, each of which were treated independently. For special purposes, such as for prediction of erythema from ultraviolet or for consideration of narrow band or spectrally selective detectors, this spectral detail, too voluminous to be presented here, can be recovered from the stored results of these calculations. The authors will endeavor to provide such information upon request.[1]

3. Conclusion

In this paper, we have presented results of an extensive theoretical investigation aimed at evaluating the effect of increasing the imaginary part of the refractive index of the aerosol material ($m=1.5-0i$ to $1.5-0.01i$) on the depletion and scattering of solar radiation in two realistic models of the terrestrial atmosphere. As expected, increased absorption due to aerosols does result in a significant decrease in the planetary albedo. We also find a decrease in the diffuse sky flux reaching the surface. Because of differential distribution of gases and aerosols, an increase in the amount of energy absorbed is not distributed evenly throughout the atmosphere. Consequently, an increase in the atmospheric dust may lead to cooling or heating depending upon the scattering and absorbing characteristics of the aerosol substance, and upon the location of dust within the atmosphere (Charlson and Pilat, 1969; Mitchell, 1971).

REFERENCES

Braslau, N., and J. V. Dave, 1972: Effect of aerosols on the transfer of solar energy through realistic model atmospheres, Part II: Partly-absorbing aerosols. Rept. RC 4152, IBM Thomas J. Watson Research Center, Yorktown Heights, N. Y.

——, and ——, 1973a: Effect of aerosols on the transfer of solar energy through realistic model atmospheres. Part I: Non-absorbing aerosols. *J. Appl. Meteor.*, **30**, 601–615.

——, and ——, 1973b: Effect of aerosols on the transfer of solar energy through realistic model atmospheres, Part III: Ground level fluxes in the biologically active bands, 0.2850–0.3700 μm. Rept. RC4308, IBM Thomas J. Watson Research Center, Yorktown Heights, N. Y.

Charlson, R. J., and M. J. Pilat, 1969: Climate: The influence of aerosols. *J. Appl. Meteor.*, **8**, 1001–1002.

Deirmendjian, D., 1969: *Electromagnetic Scattering on Spherical Polydispersions*. New York, Elsevier Publ. Co., 290 pp.

McClatchey, R. A., R. W. Fenn, J. E. A. Selby, J. S. Garing and F. E. Volz, 1970: Optical properties of the atmosphere. AFCRL-70-0527, Air Force Cambridge Research Laboratories, Bedford, Mass.

Mitchell, J. M. Jr., 1971: The effect of atmospheric aerosols on climate with special reference to temperature near the earth's surface. *J. Appl. Meteor.*, **10**, 703–714.

[1] Spectral detail of ground-level ultraviolet fluxes is now available in Braslau and Dave (1973b).